JACS
JOURNAL OF THE AMERICAN CHEMICAL SOCIETY

Communication

pubs.acs.org/JACS

Galvanic Replacement-Free Deposition of Au on Ag for Core–Shell Nanocubes with Enhanced Chemical Stability and SERS Activity

Yin Yang,[†,§] Jingyue Liu,[‡] Zheng-Wen Fu,[§] and Dong Qin*[,†]

[†]School of Materials Science and Engineering, Georgia Institute of Technology, Atlanta, Georgia 30332, United States
[‡]Department of Physics, Arizona State University, Tempe, Arizona 85287, United States
[§]Department of Materials Science, Fudan University, Shanghai, 200433, P. R. China

Supporting Information

ABSTRACT: We report a robust synthesis of Ag@Au core–shell nanocubes by directly depositing Au atoms on the surfaces of Ag nanocubes as conformal, ultrathin shells. Our success relies on the introduction of a strong reducing agent to compete with and thereby block the galvanic replacement between Ag and $HAuCl_4$. An ultrathin Au shell of 0.6 nm thick was able to protect the Ag in the core in an oxidative environment. Significantly, the core–shell nanocubes exhibited surface plasmonic properties essentially identical to those of the original Ag nanocubes, while the SERS activity showed a 5.4-fold further enhancement owing to an improvement in chemical enhancement. The combination of excellent SERS activity and chemical stability may enable a variety of new applications.

Silver nanocrystals have fascinating optical properties known as localized surface plasmon resonance (LSPR), which is essential to applications for surface-enhanced Raman scattering (SERS), optical sensing, and bioimaging.[1] Silver nanocubes, in particular, have strong electromagnetic field enhancements at their sharp corners, which can drastically increase the Raman scattering cross sections of molecules at these sites for SERS detection and imaging.[2] However, the susceptibility of elemental Ag to oxidation often leads to corner truncation and thus deterioration of SERS activity. The toxicity of the released Ag^+ ions also limits the SERS application of Ag nanocubes in a biological system. In contrast, Au is well-known for its resistance to oxidation and excellence in biocompatibility,[3] but its performance in SERS and other plasmonic applications is worse than Ag by an order of magnitude.[4] In principle, by depositing a conformal, thin shell of Au on the surface of a Ag nanocube, one would create a Ag@Au core–shell nanocube with excellence in both chemical stability (from the Au shell) and SERS activity (from the Ag core).

One approach to the formation of Ag@Au nanocube is to epitaxially deposit Au atoms on the surface of a Ag nanocube in a fashion similar to seeded growth. Since the original work by Murphy and others,[5] seeded growth has emerged as a prevalent route to the syntheses of nanocrystals from a number of noble metals, such as Ag,[6] Au,[7] Pd,[8] and Pt,[9] as well as some of their bimetallic combinations.[10] Despite the remarkable success, the capability of seeded growth is still restricted to two metals with no galvanic replacement between them. As reported by many groups,[11] a galvanic reaction will occur instantaneously when Ag nanocubes are mixed with $HAuCl_4$ in an aqueous solution, even at a temperature approaching 0 °C.[12] Hence, it has been difficult to generate Ag@Au nanocubes using seeded growth.

Several groups have attempted to solve this problem by retarding the galvanic reaction between Ag and $HAuCl_4$.[13] Table S1 shows a summary of previous studies, with details on the experimental conditions and resultant structures. Among them, Yin reported the generation of Au-coated Ag nanoplates by decreasing the reduction potential of Au^{3+} through complexation with I^- ions.[13a] However, small voids could still be observed on the surfaces of their Au-coated Ag nanoplates, suggesting the involvement of galvanic reaction. Mirkin reported the deposition of corrugated Au on Ag nanoprisms by using ascorbic acid (AA) as a reducing agent and cetyltrimethylammonium bromide (CTAB) as a capping agent.[13b] They found that galvanic replacement occurred at the corners of Ag nanoprisms even in the presence of AA and NaOH. By replacing AA with hydroxylamine (HyA), Xue reported the formation of Au-coated Ag–Au alloy nanoprisms. In this case, galvanic reaction still occurred, but the Ag^+ ions dissolved through galvanic reaction were reduced back to Ag atoms by HyA and redeposited onto the Ag nanoprisms.[13c] Most recently, Kitaev demonstrated the use of galvanic replacement for depositing uniform layers of Au on the surfaces of Ag decahedra and pentagonal nanorods with enhanced chemical stability and plasmonic properties.[13e] They used a slow injection rate and a dilute concentration for the $HAuCl_4$ solution over a period of 12 h to avoid any possible formation of pits or voids in the Ag templates. When higher injection rates and higher concentrations were used, however, they were unable to completely block the galvanic reaction by adjusting other experimental parameters, including the use of mild reducing agents, complexing agents, and varying the pH of the reaction solution. Also, there was no direct evidence such as atomic-resolution TEM images to demonstrate the formation of a conformal shell of Au on the surface of the Ag nanostructure.

Here, we report the galvanic replacement-free deposition of Au on Ag nanocubes in an aqueous solution by introducing a fast parallel reduction by AA to compete with and thereby block the galvanic reaction. By simply increasing the pH to optimize the reduction power of AA, the added $HAuCl_4$ was exclusively reduced by AA before it could participate in the galvanic reaction with Ag nanocubes. As a result, the newly formed Au atoms were

Received: March 11, 2014
Published: May 23, 2014

dx.doi.org/10.1021/ja502472x | J. Am. Chem. Soc. 2014, 136, 8153–8156

conformally deposited on the surfaces of Ag nanocubes to generate Ag@Au core–shell nanocubes. By increasing the amount of $HAuCl_4$ added into the solution, we could control the thickness of the Au shell from three to six atomic layers. With a thickness of three atomic layers (0.6 nm), the Au shell could effectively protect the Ag core to preserve its LSPR properties in an oxidative environment. Because of the stronger adsorption of probe molecules on the Au relative to Ag, the Ag@Au nanocubes exhibited a SERS enhancement factor stronger than that of Ag nanocubes. This approach worked well for Ag nanocubes with various sizes.

When $HAuCl_4$ is introduced into an aqueous suspension of Ag nanocubes in the presence of a reducing agent such as AA, it will be reduced to generate Au atoms through two parallel reactions involving Ag and AA, respectively. The reduction by Ag is a galvanic reaction (with a rate of R_{gal}) that will lead to the formation of a hollow structure whereas the reduction by AA (with a rate of R_{red}) will result in the formation of a conformal Au shell on the Ag nanocube. As illustrated in Figure 1, the final

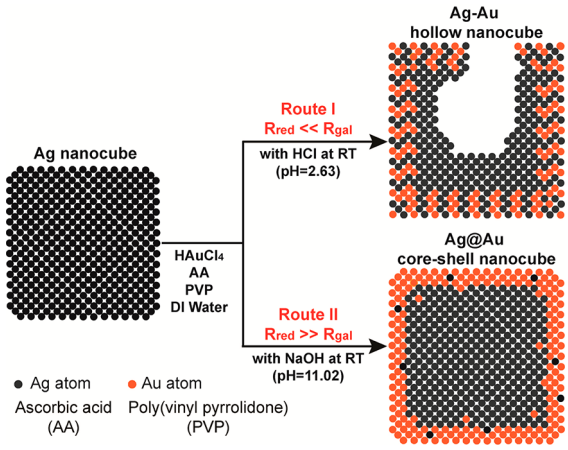

Figure 1. Schematic illustration of the two possible routes and products for syntheses that involve Ag nanocubes and $HAuCl_4$ in the presence of a weak (Route I) and strong (Route II) reducing agent based on AA at different pH values. The structure of the product is determined by the AA reduction rate (R_{red}) relative to the galvanic reaction rate (R_{gal}).

product is determined by the relative magnitudes of these two reaction rates. When $R_{red} \ll R_{gal}$, galvanic reaction dominates, generating a hollow nanocube with a thin layer of Au–Ag alloy on the surface (Route I).[14] Alternatively, when $R_{red} \gg R_{gal}$, the Au atoms are epitaxially deposited on the Ag nanocube, leading to the formation of Ag@Au nanocube (Route II). Because the $HAuCl_4$ is titrated into the reaction solution at a slow rate, self-nucleation is eliminated to promote the conformal deposition of Au atoms only on the surface of Ag nanocube. It has been reported that the reducing power of AA can be greatly enhanced by increasing the pH of reaction solution.[15] We can keep R_{gal} and manipulate R_{red} by adjusting the pH of the solution to control the reaction pathway and thus the structure of final product.

In the first set of experiments, we used Ag nanocubes of 38.0 nm in average edge length, together with slightly rounded corners (Figure S1A). Typically, we dispersed the Ag nanocubes in an aqueous solution containing poly(vinylpyrrolidone) (PVP, a capping agent and stabilizer) and AA (10 mM), followed by the introduction of 0.4 mL $HAuCl_4$ solution (0.1 mM) using a syringe pump at room temperature. When the pH was adjusted to 2.63 with the addition of HCl, we observed voids in the Ag nanocubes (Figure S1C). Upon removal of the pure Ag remaining in the nanocubes with 2.3% aqueous H_2O_2, we noticed the formation of Ag–Au hollow nanocubes with multiple pores in the walls (Figure S1D). These results suggest that galvanic reaction dominated in an acidic solution because of $R_{red} \ll R_{gal}$, which is consistent with the previous findings.[14] In contrast, when the pH was increased to 11.02 with the addition of NaOH, we obtained Ag@Au core–shell nanocubes with a well-preserved cubic shape (Figure 2A). The average edge length of

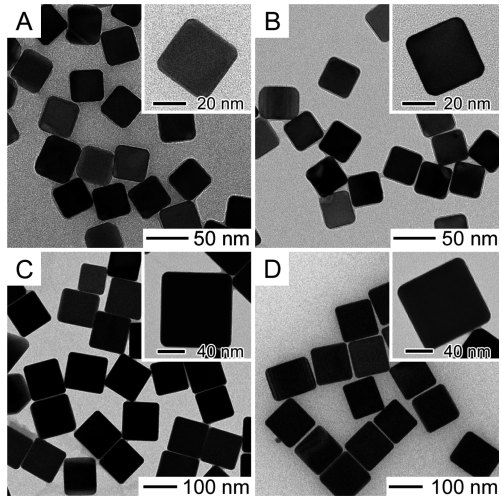

Figure 2. TEM images of Ag@Au nanocubes before (left panel) and after (right panel) incubation with 2.3% aqueous H_2O_2. The samples were prepared from (A, B) 38 and (C, D) 106 nm Ag cubes.

the Ag nanocubes was increased from 38.0 to 39.2 nm, and no void was observed in the final products. To confirm the formation of complete Au shells on the Ag nanocubes, we incubated the as-prepared samples with an excess amount of a 2.3% aqueous solution of H_2O_2, and no morphological changes was observed for a period up to 2 h (Figure 2B). We also extended the Au coating procedure to Ag nanocubes with an edge length of 106.5 nm (Figure S1B). Upon deposition of Au shells, the cubic shape was retained, while the edge length was increased to 108.0 nm (Figure 2C). Again, the Ag@Au nanocubes were stable in the aqueous solution of H_2O_2 for a period of at least 2 h (Figure 2D).

We also replaced the AA/NaOH combination with another strong reducing agent such as $NaBH_4$ and performed a similar synthesis with the 38.0 nm Ag nanocubes. As anticipated, the Au atoms were uniformly deposited on the surfaces of Ag nanocubes to generate Ag@Au nanocubes (Figure S2A). When mixed with the aqueous H_2O_2, no change was observed for the structure and shape for a period of at least 2 h (Figure S2B). These results confirm that the rapid reduction of $HAuCl_4$ by a strong reducing agent could completely suppress the galvanic reaction between Ag nanocubes and $HAuCl_4$, leading to the generation of conformal, thin shells of Au on the surfaces of Ag nanocubes.

It is important to note that pH plays an important role in regulating R_{red} and ultimately achieving galvanic replacement-free deposition of Au on Ag nanocubes. For example, when the 38 nm Ag nanocubes were dispersed in an aqueous solution containing 0.5 mL of AA (10 mM), 0.1 mL of NaOH (200 mM), and 2 mL of PVP (1 mM), we found that the titration of $HAuCl_4$ (0.1 mM) resulted in a constant decrease in pH for the reaction solution (Figure S3A). At 0.6 mL (pH = 9.69), galvanic

dx.doi.org/10.1021/ja502472x | J. Am. Chem. Soc. 2014, 136, 8153–8156

replacement was still inhibited as indicated by the absence of voids (Figure S3B). However, with the addition of 0.8 mL of $HAuCl_4$ (pH = 9.54), we observed voids at the corners of nanocubes (Figure S3C).

We also investigated the role of AA concentration in affecting R_{red} and thereby the outcome of a synthesis. Specifically, we performed another set of experiment to keep other reaction parameters unaltered, except for the use of 100 mM AA and 0.5 mL of NaOH to adjust the initial pH to 11.60. During the titration of $HAuCl_4$, we also observed a constant decrease in pH (Figure S4A). In this case, no voids were observed in the nanocubes at 0.8 mL (pH = 9.71) but they appeared at 1.0 mL (pH = 9.12) (Figure S4B,C). Collectively, our results confirm the dominating role of pH, and we concluded that the reduction of $HAuCl_4$ by AA at pH 9.5 and above could completely suppress the galvanic reaction, leading to the generation of conformal, thin shells of Au on the surfaces of 38 nm Ag nanocubes.

We used aberration-corrected high-angle annular dark-field scanning TEM (HAADF-STEM) to characterize the Ag@Au nanocubes. When $R_{red} \gg R_{gal}$, the thickness of the Au shell could be increased by increasing the amount of $HAuCl_4$ added. Figure 3A,C, shows HAADF-STEM images of two different samples of

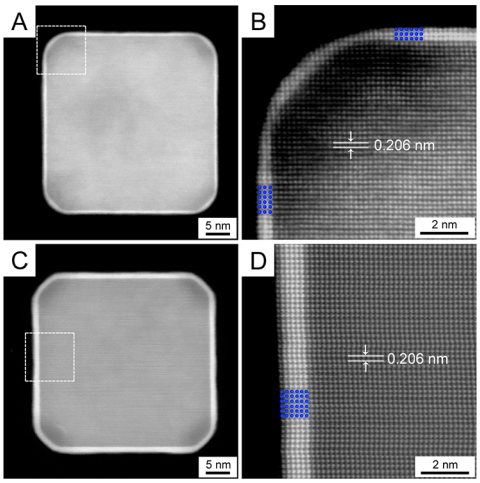

Figure 3. HAADF-STEM images taken from two samples of Ag@Au nanocubes where the Au shells were (A, B) three and (C, D) six atomic layers, respectively, in thickness.

Ag@Au nanocubes prepared using 0.4 and 0.8 mL of $HAuCl_4$, respectively. The contrast between the Au shell and Ag core can be attributed to the difference in atomic number between Ag and Au. We clearly observed the difference in Au thickness. When the nanocube was titled to the [001] zone axis, the atomic-resolution HAADF-STEM image (Figure 3B,D) offered details of the atomic arrangement for the columns of Au and the Ag atoms. On average, three and six atomic layers of Au were deposited for these two samples. The outmost surface layer of Au may not be complete, resulting in a slightly dark image contrast. There might be some interatomic diffusion between Ag and Au (as illustrated in Figure 1), but it is extremely difficult, if not impossible, to quantify the composition of the coating layer, especially the outmost surface layer.

We used UV−vis spectroscopy to characterize the LSPR properties of the Ag@Au nanocubes. Previous studies reported that the LSPR peaks of Ag−Au bimetallic nanoparticles were considerably broader than those of pure Ag or Au nanoparticles because of scattering at the interface between these two metals and frequency dependence of the dielectric constants.[16] However, when compared with the Ag nanocubes, we found that the LSPR peak of the Ag@Au nanocubes with three atomic layers of Au only showed negligible broadening in peak width, together with a slight red-shift from 435 to 443 nm (Figure 4A).

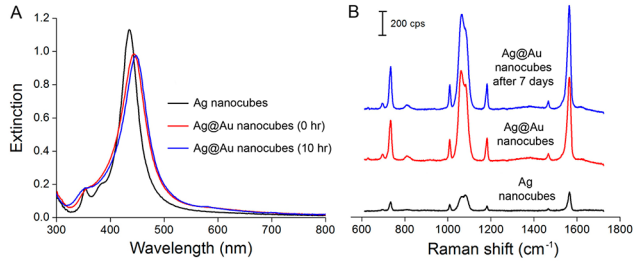

Figure 4. (A) UV−vis spectra taken from the Ag nanocubes, and the Ag@Au nanocubes before and after mixing with 2.3% aqueous H_2O_2 for 10 h. (B) SERS spectra recorded from aqueous suspensions of the 1,4-BDT-functionalized Ag nanocubes and Ag@Au nanocubes, respectively.

Our results suggest that an ultrathin shell of Au would not cause significant changes to the dielectric constants. The slight red-shift in the peak position likely arose from an increase in edge length upon Au deposition. We also used UV−vis to monitor the stability of the Ag@Au cubes when they were exposed to a strong oxidant. It was found that the LSPR peak was only red-shifted from 443 to 447 nm, while the peak intensity remained the same upon mixing with 2.3% aqueous H_2O_2 for 10 h. In comparison, the Ag nanocubes were completely etched within 3 min (Figure S5).[14b] The Ag@Au nanocubes also showed good chemical stability when they were incubated with 1.0 μM aqueous solution of NaHS for 2 days (Figure S6). These results indicate that the Ag@Au nanocubes embrace LSPR properties essentially identical to Ag nanocubes, whereas their chemical stability in an oxidative environment is greatly improved.

We evaluated the SERS activity of the Ag@Au nanocubes by benchmarking against the Ag nanocubes. To exclude any possible contribution to SERS from particle aggregation in the solution, we collected UV−vis spectra from the nanocubes before and after they had been functionalized with 1,4-benzenedithiol (1,4-BDT). As shown in Figure S7, the LSPR peak of the functionalized Ag@Au nanocubes was only red-shifted by 13 nm because of changes to the surface. No shoulder peak next to the major LSPR peak was observed, indicating that aggregation was negligible. To avoid plasmon dephasing associated with the interband transition of Au at 2.5 eV (~500 nm), we collected SERS spectra using 785 nm excitation.[17] Figure 4B shows the SERS spectra of 1,4-BDT adsorbed on the surfaces of the 38 nm Ag nanocubes and the corresponding Ag@Au nanocubes with three atomic layers of Au. Based on a reported protocol,[18] we employed the SERS peak at 1565 cm^{-1} to calculate the SERS enhancement factor (EF). When determining the number of molecules probed in SERS, it was assumed that the surface was covered by a complete monolayer of 1,4-BDT molecules with a footprint of 0.54 nm.[19] As a result, the calculated value represents a theoretical maximum number of molecules and thereby the EF reported here should be an underestimate of the actual value. The EF of the Ag@Au nanocubes was calculated to be 9.7×10^5, 5.4-fold stronger than that of the Ag nanocubes, 5.4- and 5.7-fold greater than the values previously reported for Ag concave octahedra[20] and dimers of Ag nanospheres in the solution phase,[21] respectively.

dx.doi.org/10.1021/ja502472x | J. Am. Chem. Soc. 2014, 136, 8153−8156

To understand the higher SERS activity of Ag@Au nanocubes than that of Ag nanocubes, we evaluated the contributions from both electromagnetic (EM) and chemical (CHEM) enhancements. Many other groups have demonstrated that the EM enhancement of Ag is ∼2−3 orders of magnitude stronger than that of Au.[22] Also, EM enhancement is considered as a long-range interaction that does not require the probe molecules to be directly attached to the metal surface.[23] As shown in Figure 4A, we found that the Ag@Au nanocubes exhibited LSPR features essentially identical to those of the Ag nanocubes. Likely, the 1,4-BDT molecules attached to the Au shell of 0.6 nm thick could still be influenced by the strong EM enhancement from the Ag core, leading to a EM-based SERS activity comparable to that of the original Ag nanocubes. On the other hand, it is documented that the Au-thiolate bonding is much stronger than that of Ag-thiolate.[24] Previous studies indicated that the charge transfer between a Au surface and the adsorbed molecules may promote stronger CHEM enhancement with a typical value in the range of 10−100.[25] The CHEM enhancement is considered to be a short-range effect that requires the probe molecules in contact with the surface of Au or Ag. In our case, the stronger binding of 1,4-BDT to the Au surface could contribute to a larger CHEM enhancement factor, leading to a further enhanced SERS EF for the Ag@Au nanocubes. Additionally, as shown in Figure 4B, we noticed that the SERS activity of 1,4-BDT on the Ag@Au nanocubes remained the same over a period up to 7 days, indicating that the chemical stability of the Au shell could be used to preserve the SERS activity.

In conclusion, we have demonstrated a strategy for depositing uniform, conformal shells of Au on the surfaces of Ag nanocubes to generate Ag@Au core−shell nanocubes with greatly enhanced chemical stability and SERS activity. As long as the reduction of $HAuCl_4$ was dominated by AA at a sufficiently high pH, the galvanic replacement could be completely blocked to generate Au shells with controllable thickness. The Au shell of three atomic layers was able to protect the Ag nanocube in the core from oxidation. The Ag@Au nanocubes embraced LSPR characteristics essentially identical to that of the Ag nanocubes, while their SERS activity was much stronger because of stronger binding of a thiolate to the Au surface for an improved CHEM enhancement.

■ ASSOCIATED CONTENT

Ⓢ Supporting Information

Experimental details and data. This material is available free of charge via the Internet at http://pubs.acs.org.

■ AUTHOR INFORMATION

Corresponding Author

dong.qin@mse.gatech.edu

Notes

The authors declare no competing financial interest.

■ ACKNOWLEDGMENTS

This work was supported by start-up funds from Georgia Tech. Y.Y. was also partially supported by the China Scholarship Council. J.L. was supported by start-up funds from the Arizona State University. We acknowledge the use of facilities in the John M. Cowley Center for High Resolution Electron Microscopy at the Arizona State University.

■ REFERENCES

(1) (a) Rycenga, M.; Cobley, C. M.; Zeng, J.; Li, W.; Moran, C. H.; Zhang, Q.; Qin, D.; Xia, Y. *Chem. Rev.* **2011**, *111*, 3669. (b) Dick, L. A.; McFarland, A. D.; Haynes, C. L.; Van Duyne, R. P. *J. Phys. Chem. B* **2002**, *106*, 853. (c) Jones, R. M.; Osberg, K. D.; Macfarlane, R. J.; Langille, M. R.; Mirkin, C. A. *Chem. Rev.* **2011**, *111*, 3736.

(2) (a) Tao, A.; Sinsermsuksakul, P.; Yang, P. *Nat. Nanotechnol.* **2007**, *2*, 435. (b) Rycenga, M.; Xia, X.; Moran, C. H.; Zhou, F.; Qin, D.; Li, Z.-Y; Xia, Y. *Angew. Chem., Int. Ed.* **2011**, *50*, 5473.

(3) (a) Cobley, C. M.; Chen, J.; Cho, E. C.; Wang, L. V.; Xia, Y. *Chem. Soc. Rev.* **2011**, *40*, 44. (b) Lim, I.-I. S.; Chandrachud, U.; Wang, L.; Gal, S.; Zhong, C.-J. *Anal. Chem.* **2008**, *80*, 6038.

(4) (a) Jakab, A.; Rosman, C.; Khalavka, Y.; Becker, J.; Trugler, A.; Hohenester, U.; Sönnichsen, C. *ACS Nano* **2011**, *5*, 6880. (b) Alvarez-Puebla, R. A. *J. Phys. Chem. Lett.* **2012**, *3*, 857. (c) Lismont, M.; Dreesen, L. *Mater. Sci. Eng., C* **2012**, *32*, 1437.

(5) (a) Jana, N. R.; Gearheart, L.; Murphy, C. J. *J. Phys. Chem. B* **2001**, *105*, 4065. (b) Sun, Y.; Gates, B.; Mayers, B.; Xia, Y. *Nano Lett.* **2002**, *2*, 165.

(6) Pietrobon, B.; McEachran, M.; Kitaev, V. *ACS Nano* **2009**, *3*, 21.

(7) (a) Sau, T. K.; Murphy, C. J. *J. Am. Chem. Soc.* **2004**, *126*, 8648. (b) Personick, M. L.; Langille, M. R.; Wu, J.; Mirkin, C. A. *J. Am. Chem. Soc.* **2013**, *135*, 3800.

(8) (a) Wang, F.; Li, C. H.; Sun, L. D.; Xu, C.-H.; Wang, J. F.; Yu, J. C.; Yan, C.-H. *Angew. Chem., Int. Ed.* **2012**, *51*, 4872. (b) Chen, Y.-S.; Hung, H.-H.; Huang, M. H. *J. Am. Chem. Soc.* **2009**, *131*, 9114.

(9) Mahmoud, M. A.; Tabor, C. E.; El-Sayed, M. A.; Ding, Y.; Wang, Z. L. *J. Am. Chem. Soc.* **2008**, *130*, 4590.

(10) (a) Rogers, J. A.; Someya, T.; Huang, Y. *Science* **2010**, *327*, 1603. (b) Yoo, H.; Millstone, J. E.; Li, S.; Jang, J.-W.; Wei, W.; Wu, J.; Schatz, G. G.; Mirkin, C. A. *Nano Lett.* **2009**, *9*, 3038. (c) Peng, Z.; Yang, H. *J. Am. Chem. Soc.* **2009**, *131*, 7542. (d) Habas, S.; Lee, H.; Radmilovic, V.; Somorjai, G. A.; Yang, P. *Nat. Mater.* **2007**, *6*, 692.

(11) (a) Sun, Y.; Mayers, B.; Xia, Y. *Adv. Mater.* **2003**, *15*, 641. (b) McEachran, M.; Keogh, D.; Pietrobon, B.; Cathcart, N.; Gourevich, I.; Coombs, N.; Kitaev, V. *J. Am. Chem. Soc.* **2011**, *133*, 8066. (c) Hong, X.; Wang, D.; Cai, S.; Rong, H.; Li, Y. *J. Am. Chem. Soc.* **2012**, *134*, 18165.

(12) Seo, D.; Song, H. *J. Am. Chem. Soc.* **2009**, *131*, 18210.

(13) (a) Gao, C.; Lu, Z.; Liu, Y.; Zhang, Q.; Chi, M.; Cheng, Q.; Yin, Y. *Angew. Chem., Int. Ed.* **2012**, *51*, 5629. (b) Sanedrin, R. G.; Georganopoulou, D. G.; Park, S.; Mirkin, C. A. *Adv. Mater.* **2005**, *17*, 1027. (c) Shahjamali, M. M.; Bosman, M.; Cao, S.; Huang, X.; Saadat, S.; Martinsson, E.; Aili, D.; Tay, Y. Y.; Liedberg, B.; Loo, S. C. J.; Zhang, H.; Boey, F.; Xue, C. *Adv. Funct. Mater.* **2012**, *22*, 849. (d) Murshid, N.; Gourevich, I.; Coombs, N.; Kitaev, V. *Chem. Commun.* **2013**, *49*, 11355.

(14) (a) Sun, Y.; Xia, Y. *J. Am. Chem. Soc.* **2004**, *126*, 3892. (b) Yin, Y.; Zhang, Q.; Fu, Z.; Qin, D. *ACS Appl.. Mater. Interfaces* **2014**, *6*, 3750.

(15) (a) Luty-Blocho, M.; Paclawski, K.; Wojnicki, M.; Fitzner, K. *Inorg. Chim. Acta* **2013**, *395*, 189. (b) Personick, M.; Mirking, C. A. *J. Am. Chem. Soc.* **2013**, *135*, 18238.

(16) (a) Wang, X.; Zhang, Z.; Hartland, G. V. *J. Phys. Chem. B* **2005**, *109*, 20324. (b) Coronado, E. A.; Schatz, G. C. *J. Chem. Phys.* **2003**, *119*, 3926.

(17) Rycenga, M.; Hou, K. K.; Cobley, C. M.; Schwartz, A. G.; Camargo, P. H. C.; Xia, Y. *Phys. Chem. Chem. Phys.* **2009**, *11*, 5903.

(18) Stiles, P. L.; Dieringer, J. A.; Shah, N. C.; Van Duyne, R. P. *Annu. Rev. Anal. Chem.* **2008**, *1*, 601.

(19) Cho, S. H.; Han, H. S.; Jang, D. J.; Kim, K.; Kim, M. S. *J. Phys. Chem.* **1995**, *99*, 10594.

(20) Xia, X.; Zeng, J.; McDearmon, B.; Zheng, Y.; Li, Q.; Xia, Y. *Angew. Chem., Int. Ed.* **2011**, *50*, 12542.

(21) Li, W.; Camargo, P. H. C.; Lu, X.; Xia, Y. *Nano Lett.* **2009**, *9*, 485.

(22) García de Abajo, F. J. *Rev. Mod. Phys.* **2007**, *79*, 1267.

(23) Schatz, G. C. *Acc. Chem. Res.* **1984**, *17*, 370.

(24) Ulman, A. *Chem. Rev.* **1996**, *96*, 1533.

(25) (a) Morton, S. M.; Jensen, L. *J. Am. Chem. Soc.* **2009**, *131*, 4090. (b) Wu, D.-Y.; Liu, X.-M.; Duan, S.; Xu, X.; Ren, B.; Lin, S.-H.; Tian, Z.-Q. *J. Phys. Chem. C* **2008**, *112*, 4195. (c) Valley, N.; Greeneltch, N.; Van Duyne, R. P.; Schatz, G. C. *J. Phys. Chem. Lett.* **2013**, *4*, 2599.